

## Significant issues posed by the 2016 Kumamoto earthquake with regard to active fault assessment and disaster mitigation

\*Yasuhiro Suzuki<sup>1</sup>

1. Nagoya University

After the Kumamoto earthquake, it was necessary to critically examine the efficiency of evaluation by the Headquarters for Earthquake Research Promotion of Japan for implementation of disaster mitigation countermeasures. Was the headquarters successful in predicting the earthquake? Was the information provided by the headquarters effective in mitigating damages? What should the headquarters and research institutes learn from this earthquake?

Many residents in Kumamoto said that they knew the existence of the Futagawa-Hinagu fault and were aware that the probability of an earthquake was “relatively higher,” prior to the earthquake. This can be regarded as a significant achievement for the headquarters after having devoted 22 years since 1995 to predict the occurrence of an earthquake. However, there is doubt whether these efforts actually led the residents to employ countermeasures.

The behavior of the fault during the Kumamoto earthquake was not consistent with the fault classification assumed in the evaluation. Another remarkable feature of the Kumamoto earthquake was that the "severely damaged zones" were generated along the active fault. A seismic intensity of 7 was recognized officially only in Mashiki town and Nishihara village. However, severe damages indicated that the seismic intensity in most areas along the earthquake fault was equivalent to 7. Although the Ministry of Land, Infrastructure and Transport issued a policy to not revise the Building Standards Law, the current standard is regarded only as a minimum requirement, and is not sufficient for a seismic intensity of 7. This leads to the conclusion that there should be a need to identify areas where the seismic intensity could reach 7.

In addition, various surface ruptures were generated during the Kumamoto earthquake. There were (1) narrowly defined earthquake faults, which were judged to be surface appearances of the seismic fault itself, (2) secondary faults induced with the seismic faulting, (3) gravitating landslides having no relation with the seismic fault. Are they clearly distinguishable at present? It is important to clarify the mechanism of ruptures and improve the hazard assessment of various ground displacements.

There were several unsolved problems such as determining a relationship between damages and faulting, even in the 1995 Hanshin Awaji earthquake. One of the reasons as to why these problems were unsolved is the lack of inter-disciplinary research. After the Kumamoto earthquake, it is necessary to develop a new inter-disciplinary research promotion system, considering all the risks posed by the earthquake.

Keywords: Kumamoto earthquake, active faults assessment, disaster mitigation

## Landslides in urban residential region induced by the 2016 Kumamoto earthquake

\*Toshitaka Kamai<sup>1</sup>, Issei Doi<sup>1</sup>, Gonghui Wang<sup>1</sup>

1. Disaster Prevention Research Institute, Kyoto University

Recent destructive earthquakes in urban regions, such as the 1978 Miyagiken-oki earthquake the 1995 Kobe earthquake, and the 2011 Tohoku earthquake have destabilized many of the gentle slopes in residential areas around large cities in Japan. Beyond the serious danger to residents of the earthquake affected areas, these landslides revealed the weaknesses of urban development in cities of Japan. The 2016 Kumamoto earthquake induced serious damages in the suburbs of Kumamoto city. The strong motion along the earthquake fault across the urban region caused slope damages, that are building deconstruction, collapse of houses, and landslides of artificial steep slopes, but also the ground condition controlled their distribution and landslide mechanism.

Keywords: Fill, Residential developments

# Building Damage on Surface Faulting of 2016 Kumamoto Earthquake, and Counter Measures

\*Yoshiaki Hisada<sup>1</sup>

1. Kogakuin University, School of Architecture

This paper reports the results for investigating building damage near the surface faulting of the 2016 Kumamoto earthquake, and counter measures of building. The results of the building investigation indicated that most of severe damage occurred in those directly above the surface faulting, because of its slip deformation. And, almost all severe damaged buildings were very old wooden houses/apartments, whereas new wooden or RC buildings showed very minor damage. In the Shimojin area, for examples, the ground motion was probably not strong enough to cause severe damage, and thus, the highest damage was Grade 3. All of them were very old wooden buildings and directly above the surface faulting. Even though the best counter measure for buildings near active faults is to avoid them, it is unrealistic to prohibit regular buildings in such areas shown in this study, because the exact locations of the surface faulting are very difficult to identify. In fact, they differed from those of the actual surface faulting, because of the young alluvial/volcanic sediments and the artificial land development. In addition, the recurrence intervals of the active faults are extremely long (usually several thousand years), as compared with the lifetime of a building. And the most importantly, various safety counter measures are effective, even for the building directly above the surface faulting. For example, the new wooden houses with the mat foundation of RC could prevent the slip deformation from reaching the building, and the combinations of the shear wall and light roofs prevented severe damage. On the other hand, the old Japanese traditional houses generally suffered severe damage, but their structural flexibilities could prevent collapsing by following the slip deformation. The collapsed buildings were generally very old and lacked both the sufficient earthquake-resisting structural members and the effective connections among them.

Keywords: 2016 Kumamoto Earthquake, Surface Faulting, Damage and Counter Measures of Building

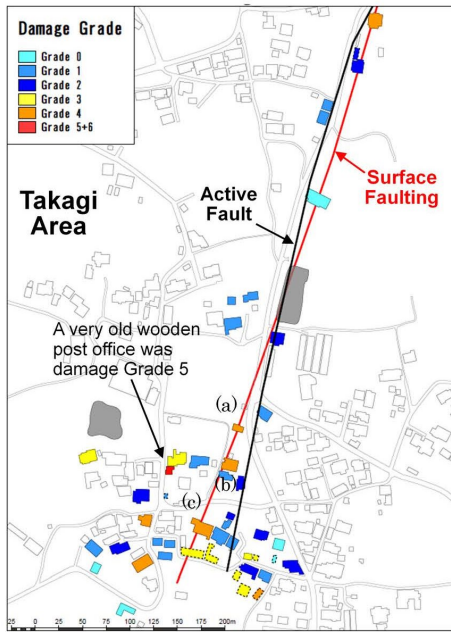


図1 地表地震断層近傍の建物被害分布 (高木地区)

表1 地表地震断層近傍の建物被害統計 (高木地区)

構造	棟数	割合	築年	棟数	割合
木造	35	90%	30年以上	17	44%
S造	3	8%	30~10年	12	31%
RC造	1	3%	10年以下	10	26%
合計	39	100%	合計	39	100%

古い建物			非常に古い建物		
被害度	棟数	割合	被害度	棟数	割合
Grade 0	0	0%	Grade 0	0	0%
Grade 1	6	50%	Grade 1	5	29%
Grade 2	3	25%	Grade 2	5	29%
Grade 3	1	8%	Grade 3	2	12%
Grade 4	2	17%	Grade 4	4	24%
Grade 5	0	0%	Grade 5	1	6%
Grade 6	0	0%	Grade 6	0	0%
合計	12	100%	合計	17	100%
全壊	2	17%	全壊	5	29%
倒壊	0	0%	倒壊	1	6%

断層直上のみ			断層直上以外		
被害度	棟数	割合	被害度	棟数	割合
Grade 0	1	14%	Grade 0	3	9%
Grade 1	1	14%	Grade 1	15	47%
Grade 2	2	29%	Grade 2	7	22%
Grade 3	0	0%	Grade 3	3	9%
Grade 4	3	43%	Grade 4	3	9%
Grade 5	0	0%	Grade 5	1	3%
Grade 6	0	0%	Grade 6	0	0%
合計	7	100%	合計	32	100%
全壊	3	43%	全壊	4	13%
倒壊	0	0%	倒壊	1	3%



(1) 古い在来木造住宅 (2) 新しい軽量鉄骨住宅 (3) 非常に古い伝統木造住宅

写真1 御船町高木地区における地表地震断層直上の建物被害の例

# Consideration of uncertainty in strong-motion prediction and seismic hazard analysis

\*Hiroyuki Fujiwara<sup>1</sup>, Nobuyuki Morikawa<sup>1</sup>, Asako Iwaki<sup>1</sup>, Takahiro Maeda<sup>1</sup>

1. National Research Institute for Earth Science and Disaster Resilience

The Kumamoto earthquakes were earthquakes that were long-term evaluated by the headquarters of earthquake research promotion of Japan. The earthquakes occurred in a part of the Futagawa fault zone and the Hinagu fault zone where the seismic hazard maps with specified seismic source fault were published. Based on the knowledge obtained from the analysis of the Kumamoto earthquake, we will consider problems in strong-motion prediction and seismic hazard analysis, especially handling of uncertainty in prediction of future events. We classify the uncertainty in assessment into aleatory variability and epistemic uncertainty. The aleatory variability is evaluated as a random variable, and the epistemic uncertainty is evaluated using a logic tree.

(1) Consideration of uncertainty in setting earthquake magnitude (seismic moment)

a) Consideration of epistemic uncertainty about the concept of model setting of fault geometry

Considering the epistemic uncertainty with respect to the setting of the size of source fault, it is necessary to consider the following model in addition to the basic model according to the current 'recipe' .

1) Model assuming that the source fault length is longer than the surface fault length.

2) Model assuming that depth of lower end of fault slightly deeper than the lower limit of the seismogenic layer.

3) Model with the top of the source fault at 0 km (ground).

4) Model considering uncertainty in setting dip angle.

b) Consideration of uncertainty concerning outer source fault parameters

It is important to properly consider the epistemic uncertainty accompanying the selection of the equation and the aleatory variability included in the prediction in parameter setting of the source fault model using the empirical formula.

1) Epistemic uncertainty on selection of empirical formula in L-Mo relation and Mj-Mw relation.

2) Aleatory variability in Mo-S relation and Mo-A relation.

(2) Consideration of uncertainty in modeling position and shape of source fault

In the strong-motion evaluation, the emphasis was mainly on modeling of short period strong-motion generation, the source fault was within the seismogenic layer, and its upper end was not 0 km (surface). In order to predict the strong ground motion in the very vicinity of the fault, detailed modeling of the position and shape of the source fault with the top end depth of 0 km is necessary. It is necessary to consider the uncertainty concerning detailed modeling of position and shape.

(3) Consideration of uncertainty in inner parameters of source fault model

In the strong-motion prediction by simulation using the fault model, it is necessary to evaluate both "average ground motion level" and "variation of ground motion due to model uncertainty". For that purpose, it is necessary to consider the uncertainty in the inner parameters of source fault model. It is important to consider the uncertainty concerning starting point of rupture, asperity position, inhomogeneity of effective stress of asperity, the setting of slip velocity time function in the shallower part than the seismogenic layer. In the prediction using simulation, it is necessary to clarify relationship

between the reproduction model of the past earthquake and the model for prediction.

(4) Consideration of uncertainty in subsurface structure model

The uncertainty of underground structure model is hardly considered compared with the modeling of source fault. A model based on dense observation data is being developed in the land area, but there is large uncertainty in the ocean floor area. In order to cover up to about 1 to 2 Hz, it is necessary to consider aleatory variability due to random inhomogeneities. In the evaluation of the amplification factor by the shallow ground, consideration of the epistemic uncertainty due to the lack of data is a future subject.

(5) Consideration one size smaller earthquakes than the characteristic earthquake

The earthquake on April 14 (M6.5), which is thought to be a smaller earthquake than the characteristic one, but the maximum seismic intensity 7 is observed. Modeling magnitude and occurrence frequency of smaller earthquakes than the characteristic one is an important issue.

Keywords: strong-motion prediction, seismic hazard analysis, uncertainty, variability

# Reconsideration of earthquake disaster countermeasures based on the experience of the Kumamoto earthquake

\*Itsuki Nakabayashi<sup>1</sup>

1. Meiji University, Graduate School of Economic and Political Sciences

The 2016 Kumamoto earthquake caused twice strong shakes of 7 degree of JSI with interval of 28 hours. The first strong shake killed 9 people and the second shake killed 41 people in midnight. The number of earthquakes as aftershock which occurred 1 degree of JSI and more reaches more than 4,200. About 230,000 of people were evacuated in shelters due to the repeated aftershocks. As the result of it, the number of the related death reached more than of 150 persons as three times as number of the direct death victims. The experience of the Kumamoto earthquake clarified the various problem of the Japanese countermeasures for earthquake, such as evacuation system, regulation system of fault zone, anti-earthquake standard of building of important facilities, countermeasure against repeated aftershocks, care of the elderly in shelter for decrease of the related death, the supply of temporary houses, and so on in the emergency and quick recovery period, to be re-considered. This one year after the earthquake was expensed for only making a reconstruction plan, but implementing reconstruction projects for sufferers.

# S-wave velocity measurement across active faults and the effect of basin geometry on site response, California, USA

\*Koichi Hayashi<sup>1</sup>, Mitchell Craig<sup>2</sup>

1. Geometrics Inc, 2. California State University, East Bay

We measured S-wave velocity ( $V_s$ ) profiles at eleven sites in the east San Francisco Bay area using surface wave methods. The sites were placed around the Hayward fault and the Calaveras fault (Figure 1). The 30-year probabilities of magnitude 6.7 or greater earthquakes on the Hayward-Rodgers Creek and Calaveras faults have been estimated at 32 % and 25 %, respectively. These faults run through densely populated areas and knowledge of a detailed two- or three dimensional  $V_s$  structure along the faults is needed in order to estimate local site effects due to a potential earthquake. This presentation summarizes data obtained by the surface wave methods, shows  $V_s$  profiles calculated by inversion, and discusses the effect of 2D  $V_s$  structure on surface ground motion. Data acquisition included multichannel analysis of surface waves using an active source (MASW), a passive surface-wave method using a linear array of geophones (Linear-MAM), and a two station spatial autocorrelation method (2ST-SPAC) using long-period accelerometers. Maximum distance between stations ranged from several hundred meters to several kilometers, depending on the site. Minimum frequency ranged from 0.2 to 2 Hz, depending on the site, corresponding to maximum wavelengths of 10 to 1 km. Phase velocities obtained from three methods were combined into a single dispersion curve for each site. A nonlinear inversion was used to estimate  $V_s$  profiles to a depth of 200 to 2000 m, depending on the site. Resultant  $V_s$  profiles show significant differences among the sites (Figure 2). On the west side of the Hayward fault and the east side of the Calaveras fault, there is a low velocity layer at the surface, with  $V_s$  less than 700 m/s, to a depth of approximately 100 m. A thick intermediate velocity layer with  $V_s$  ranging from 700 to 1500 m/s lies beneath the low velocity layer. Bedrock with  $V_s$  greater than 1500 m/s was measured at depths greater than approximately 1700 m. Between the Hayward Fault and the Calaveras Fault, thicknesses of the low velocity layer and the intermediate velocity layer are less than 50 m and 200 m respectively, and depth to bedrock is less than 250 m. To evaluate the effect of a lateral change in bedrock depth on surface ground motion due to an earthquake, a representative  $V_s$  cross section perpendicular to the Hayward fault was constructed and theoretical amplification was calculated using a viscoelastic finite-difference method. Calculation results show that the low frequency (0.5 to 5 Hz) component of ground motion is locally amplified on the west side of the Hayward fault because of the effect of two-dimensional structure. The results of this investigation indicate that the phase velocity information obtained using the 2ST-SPAC method with a limited number of high quality sensors provides valuable  $V_s$  information over a wide depth range. It offers a robust alternative to widely-used single station methods such as the horizontal to vertical spectral ratio. Though the 2ST-SPAC method and other passive surface wave methods using an anisotropic or linear array cannot equal the performance of an isotropic array in the case of strongly anisotropic ambient noise, they do provide an effective alternative for many urban environments where ambient noise is relatively isotropic and potential sites for array deployment are limited to corridors along roadways. The inversion of surface wave data is essentially non-unique and we cannot remove uncertainty from analyses, the effect of the uncertainty depends on the purpose of investigation and the use of the data. Several different velocity profiles that yield almost the same theoretical phase velocities were examined to evaluate the effect of uncertainty of inversion on amplification calculation. The results shows that the site amplifications calculated from  $V_s$  profiles are relatively insensitive to uncertainties in the velocity profiles.



Keywords: Active fault, S-wave velocity, Surface-wave method, Micro-tremor array measurements, Site amplification, Basin edge effect

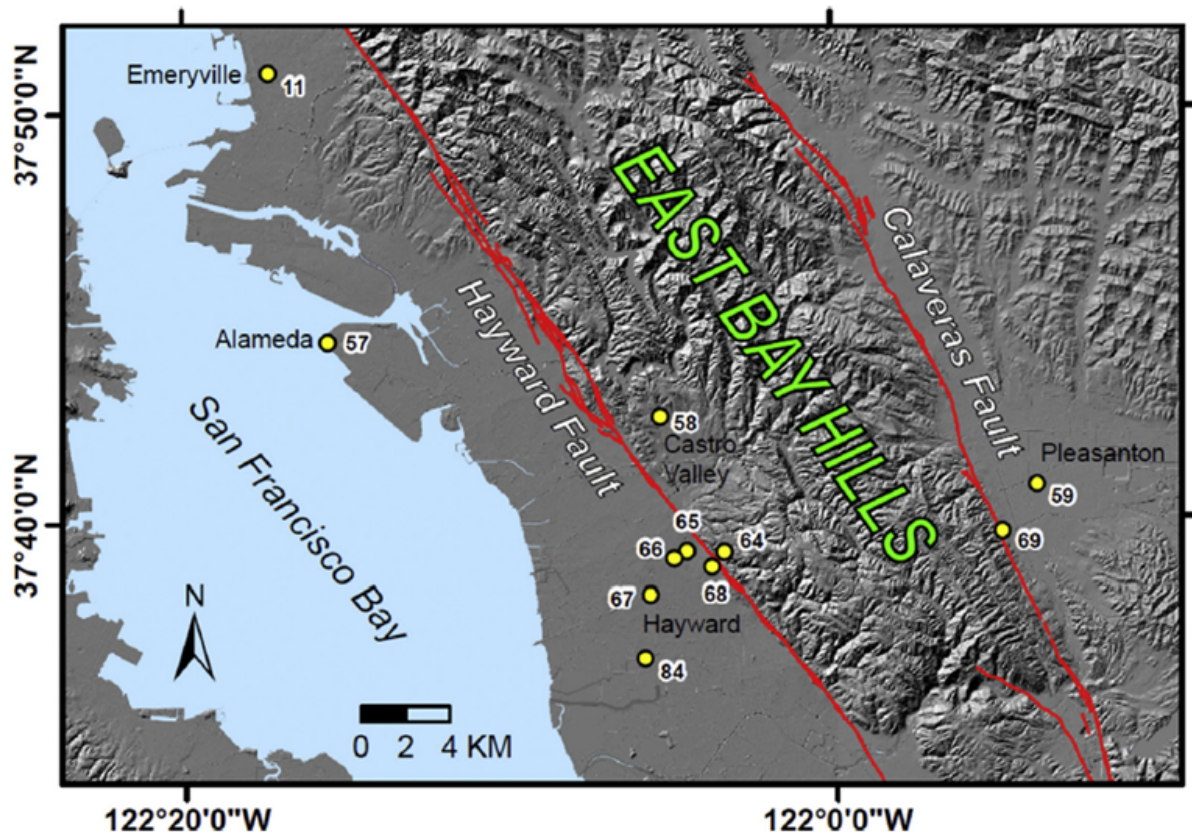


Figure 1. Sites of investigation. 11 : Emeryville, 57 : Alameda, 58 : Castro Valley, 59 : Pleasanton, 64 : CSU East Bay, 65 : Charles Ave, 66 : Huntwood Ave, 67 : Southgate Park, 68 : Cemetery, 69 : Alviso Adobe, 84 : Eden Shores Park.

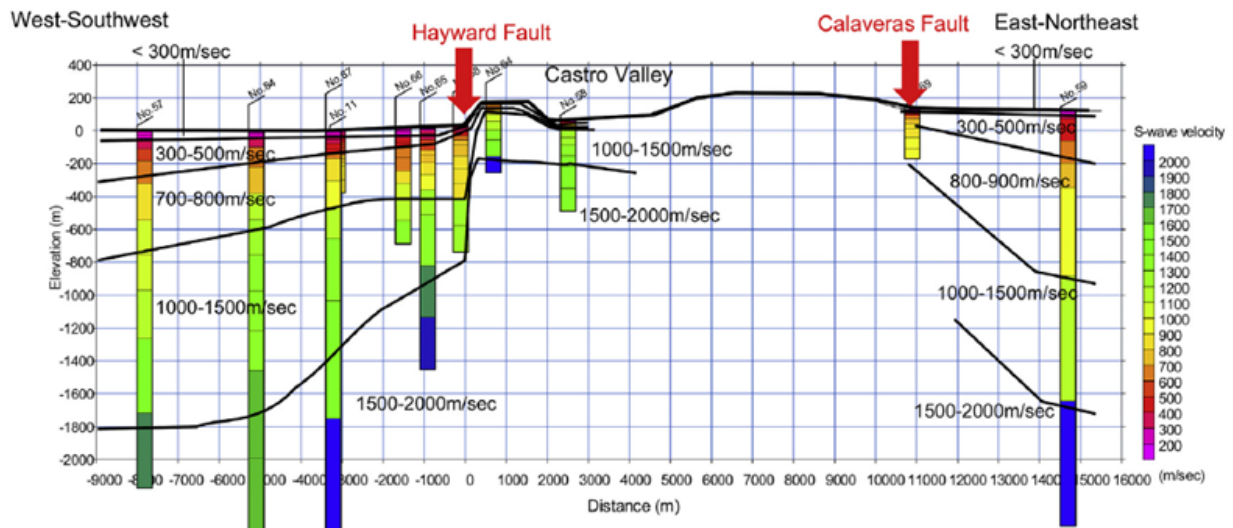


Figure 2. Schematic S-wave velocity section based on the S-wave velocity profiles obtained in this study.

# Geotechnical aspect of damage found along seismic fault that appeared in the 2016 Kumamoto Earthquake

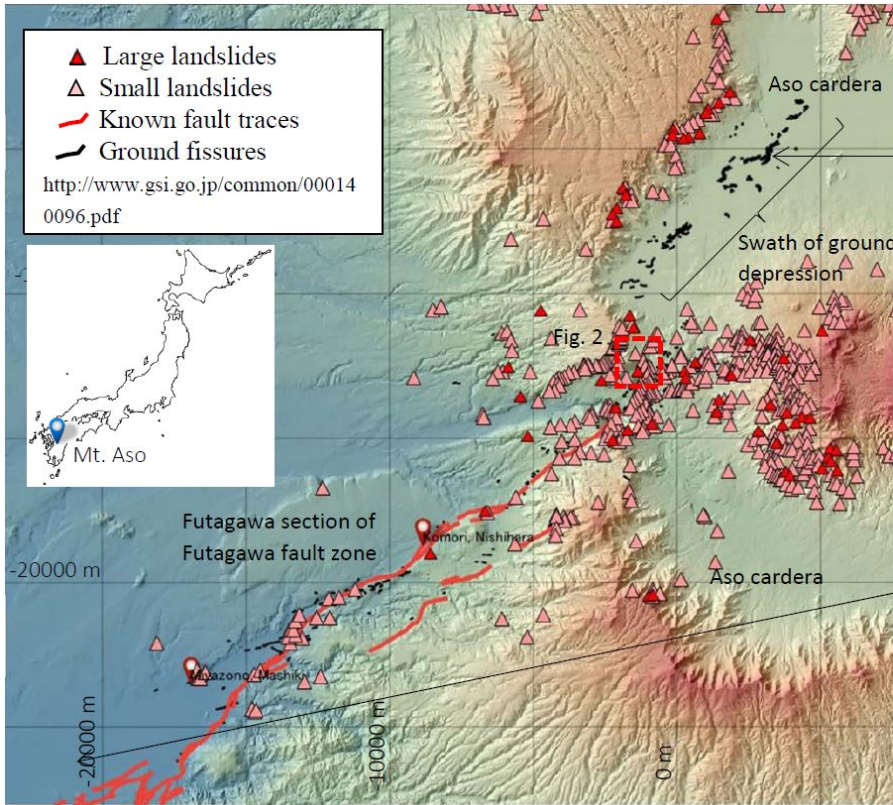
\*Kazuo Konagai<sup>1</sup>

1. Yokohama National University

Starting with a magnitude-6.5 foreshock on April 14, 2016, a series of major earthquakes including the magnitude-7.3 main shock on April 16 have hit the central Kumamoto area of Kyushu, Japan, causing deaths, injuries and widespread damage to various facilities. The activity of the fault, whose right-lateral offset appeared in the main shock along the previously known section of the Futagawa fault zone, caused extensive damage to roads, bridges, a tunnel and a dam. The observed features of the damage again showed that not only intense shakes but also ground deformations such as landslides, lateral spread of embankments and levees, soil liquefactions etc., which can be found within a swath along the fault trace, can be equally or often more responsible for devastations. Moreover close to 500 millimeters of rain fell on some parts along the quake-hit areas on June 20 and 21, causing further extensive landslides and flooding, highlighting the difficulty to cope with earthquake-flood multi hazards.

LiDAR, Laser based altimetry, can penetrate through tree canopy, revealing detailed feature of bare earth left behind by past natural hazards, and the LiDAR image of the mountain slope along the outer rim of the Aso crater shows evidence of past landslides as well as the most recent one that has hit an important location for traffic. Moreover cracks are seen along the exposed scar indicating future risk. As long as clear evidence for past large soil deformation was there in LiDAR images, landslides/active fault maps etc., we could bring potential hazard to light and take necessary actions. However these pieces of evidence can be often buried beneath surface soil deposits particularly when they are near an active volcano. Because large ground deformations can be repeated in any extreme natural events as can be seen in the past major earthquakes, they are to be recorded in a quantitative manner.

Keywords: Kumamoto Earthquake of 2016, Geotechnical hazard, earthquake-flood multi hazards



House hanging a little over the northwestern offset of the ground at N32.9568°, E131.0368



Tilted RC housing of pump for Akita clean water well No. 2 at N32.7670°, E130.7786 °: A low lying area east of this housing is found sunken by more than a meter

## Geomorphological and geological features of landslide deposits caused by the 2016 Kumamoto earthquake at the western part of Aso Volcano

\*Ken-ichi Nishiyama<sup>1</sup>, Masayuki Torii<sup>3</sup>, Mitsuru Okuno<sup>2</sup>

1. Graduate School of Science & Technology, Tokushima University, 2. Faculty of Science, Fukuoka University, 3. Graduate School of Science & Technology, Kumamoto University

The Kumamoto earthquake (Mj=7.3) on April 16, 2016 triggered many landslides at the slope of Aso Volcano. The main shock triggered more than 100 landslides of loam deposits. Earthquake-induced earthflow deposits consists of loam blocks flowed relatively long distance along the San-odani River.

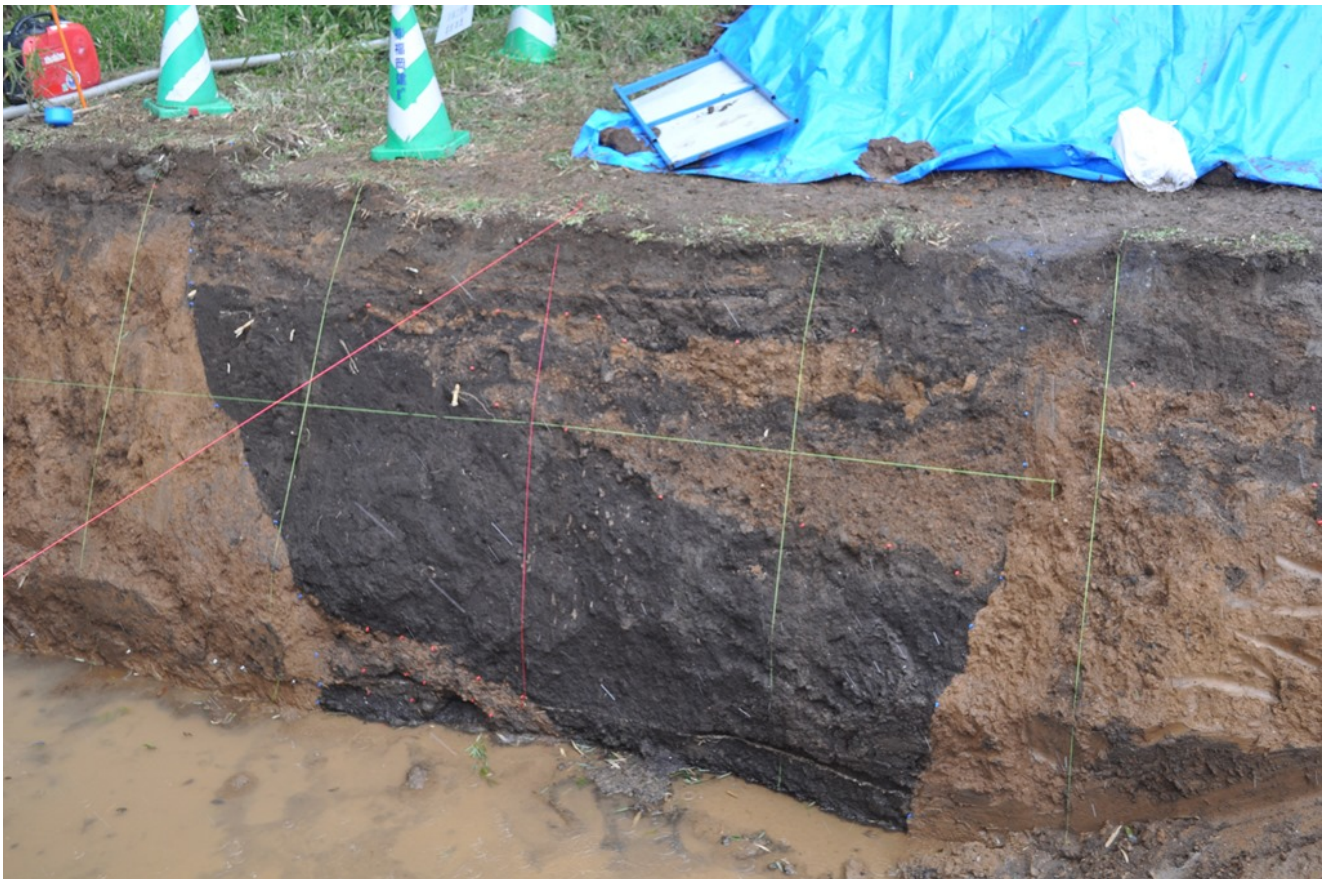
Keywords: Kumamoto earthquake, Aso volcano, landslide

## Reserach on active faults in urbanized area of Mashiki Town by the City Bureau, MLIT and its significance

\*Yohta KUMAKI<sup>1</sup>, Hiroshi Une<sup>2</sup>

1. Senshu University, 2. Geospatial Information Authority of Japan

The Urban Development and Improvement Division, City Bureau, Ministry of Land Infrastructure, Transport and Tourism researched to specify the location of active faults including pitting (see photo) in urbanized area of Mashiki Town, which utterly devastated by the Kumamoto Earthquake of 2016, for the purpose of supporting the reconstruction of urbanized area. The author introduce the result of the research and discuss the significance of the active fault reserch in the area where small surface deformations arised in urbanized area.



# Consideration of existence of active faults in the Reconstruction Plan of Mashiki Town

\*Hiroshi Une<sup>1</sup>

1. Geospatial Information Authority of Japan

The Mashiki Town, utterly devastated by the 2016 Kumamoto Earthquake, established “the Reconstruction Plan of Mashiki Town” in December 2016 aiming to revive from earthquake disaster and reconstruct disaster-proof town. The questionnaire survey to the residents which was carried out in the process of drafting of the plan revealed that a majority of the residents were in fear for the existence of active fault and the occurrence of future earthquake. In parallel with this planning, the City Bureau of Ministry of Land, Infrastructure, Transport and Tourism conducted the research and analysis of the background elements of the damage such as fault and soil condition and the consideration of measures to rebuild disaster-proof town, and provided the results to support the Town. It assumed that at least three east-west active faults run below the town center of the Mashiki Town, and proposed to take special consideration for the land use on active faults from the viewpoint of avoidance of damage risk while implementing land readjusting project in town center. Although concrete land use planning has not started yet, this is a remarkable policy based on fair understanding of the nature of active faults aiming at the coexistence with active faults.

Keywords: Reconstruction Plan of Mashiki Town, land use on active fault, coexistence with active fault

## 益城町市街地内における活断層の位置

### 層位置の推定方法

以下の4点から総合的に判断

- ①同一地層の標高差の有無
- ②明瞭な段差地形の有無
- ③活断層の繰り返しにより柔らかくなった地盤の有無
- ④地表に現れる連続的な亀裂の有無

- 益城町市街地において、3本の活断層(A・B・C)が存在。
- 今回の地震では、**活断層Aが主体に活動し、益城町市街地では、最大35cmの右ズレ及び最大15cm程度の上下変位(南落ち)を確認。**  
(活断層B,Cのズレは活断層Aに比べて微量)



国土交通省都市局(2017):「熊本地震からの益城町の市街地復興に向けた安全対策のあり方等に関する中間報告」より



## Earthquake faults along the Kiyomasa-kodo and in the northwestern part of the Aso caldera during 2016 Kumamoto Earthquake

\*Mitsuhisa Watanabe<sup>1</sup>, Takashi Nakata<sup>2</sup>, Hideaki Goto<sup>3</sup>, Kei Tanaka<sup>4</sup>, Yasuhiro Suzuki<sup>5</sup>, Keita Takada<sup>6</sup>

1. Faculty of Sociology, Toyo University, 2. Emeritus professor, Hiroshima University, 3. Graduate school of letters, Hiroshima University, 4. Japan Map Center, 5. Nagoya University, 6. Fukken Co. Ltd.

A large number of ruptures appeared along the Futaenotoge seismic zone and its extension during 2016 Kumamoto earthquake. There are right-lateral earthquake faults along the Kiyomasa-kodo (Seishoko-do). The narrow "severely damaged zone" indicates that the upper cutoff depth of seismogenic layer is very shallow. The remarkable surface ruptures aligned in ENE-WSW direction intermittently in the northwestern part of the Aso caldera. The locations of the ruptures are not coincided in space with soft grounds, and strong tremor did not attack the areas. The tectonic ruptures in the form of grabens caused the lateral ground displacements in these areas.

Keywords: earthquake fault, right-latera fault, normal fault, Kiyomasa-kodo, Aso caldera, 2016 Kumamoto earthquake

# Ground motion amplification on heavily damaged zone in the Mashiki town during the 2016 Kumamoto Earthquake

\*Hiroyuki Goto<sup>1</sup>, Masayuki Yoshimi<sup>2</sup>, Yoshiya Hata<sup>3</sup>

1. Disaster Prevention Research Institute, Kyoto University, 2. National Institute of Advanced Industrial Science and Technology, 3. Osaka University

Severe ground motion damages occurred in the downtown area of the Mashiki town, Kumamoto Prefecture, during the 2016 Kumamoto earthquake, Japan, and several heavily damaged zone appeared in the center of the downtown. Nonlinear site response for the first (14th Apr., 2016) and main shocks (16th Apr., 2016) is important factors to explain the reason why the heavily damaged zone appeared. We analyzed the soil nonlinearity by using the surface and borehole records at KiK-net KMMH16 (Mashiki) station. Optimal S-wave velocity models clearly depended on the amplitude of input ground motions. Strain dependent shear stiffness and damping ratio were estimated to explain the S-wave velocity dependence on the input motion amplitudes. We conducted nonlinear analyses at KMMH16 site on the basis of the nonlinear model. The synthetic surface ground motions agreed well with the observed ones, especially at S-wave amplitude and phase for the first and main shocks. In addition, we also conducted the same analyses at TMP3 site, which was located in the heavily damaged zones. The synthetic motions well represented the observed ones, and difference of spectral accelerations was well explained by the analyses. The results indicated that the soil nonlinearity played a big role to cause the difference of ground motions, and thus the damaged zone appeared in the downtown of the Mashiki town.

Keywords: 2016 Kumamoto Earthquake, Ground amplification, Mashiki town

# Clarification of the relationship between the damage distribution and surface cracks caused by the 2016 Kumamoto earthquake

\*Tsuyoshi Haraguchi<sup>1</sup>

1. Department of Geosciences, Graduate School of Science, Osaka City University

In the 2016 Kumamoto earthquake, catastrophic damage concentrates along active faults. At the time of the earthquake, various cracks appeared on the surface. I will discuss surface displacement and damage caused by the earthquake.

Clear surface earthquake faults appeared along the line where the active fault position was recognized before the earthquake. In the part where the fault passed, the retaining wall was broken in the range of several meters wide due to fault displacement. However, there are no houses collapsed by fault displacement. The wooden house existing on the surface earthquake fault twisted and deformed, but it did not collapse. In the old wooden house built at the point where the fault passed beside the fault, there was no falling of the roof tile and it was not damaged. The catastrophic damage concentrated in the center of Mashiki-machi. A surface earthquake fault appeared on a part of it, displacing the paved road up to 40 cm. However, the line where the surface earthquake fault appeared and the distribution of the collapsed houses are not finely matched.

A surface earthquake fault appeared also in the western part of the Aso caldera. A part of the fault displaced the houses, but the houses has not collapsed. In the Aso Valley, a linear collapse area crack occurred. Analysis of the surface displacement vector from the DEM before and after the earthquake showed that the blocks with a major diameter of 1 to 2 km moved 2 to 5 m in the north - northwest direction in the three areas along the Kurokawa river (Mukaiyama et al. 2016). As a result of the underground exploration conducted in the Matoishi which is one of the three districts, I confirmed the existence of a low velocity layer of about 10 m in thickness right under the crack. According to the testimony of the elderly, the linear cracked parts ware that the yellow soil was collected before 1940. In summary, devastating damage concentrates along the active fault in the 2016 Kumamoto earthquake. However, focusing only on damage caused by fault displacement, it was shown that the range of damage is extremely limited.

Keywords: 2016 Kumamoto earthquake, active fault

# Geometry of surface fault ruptures of the 2016 Kumamoto earthquake and house damages

\*Takashi Nakata<sup>1</sup>

1. Hiroshima University

During the Kumamoto earthquake (Mw 7.3) on April 16, 2016 severe house damages were caused by the strong shaking and surface fault rupture along active fault known as the Futagawa-Hinagu fault in central Kyushu, southwest Japan and near-by faults some of which were not known before. Main surface fault ruptures with right-lateral slip appeared along northern part of the Futagawa-Hinagu. Severe house damages appeared in narrow zones several hundred meters from the surface fault traces, and destructive house damages were unevenly distributed and concentrated in the both ends of the main surface fault rupture as observed Mashiki town and Minami-Aso village. Along the main surface fault rupture severe house damages were locally concentrated in the places where surface fault ruptures make steps and bends, while house damages were relatively small along the areas where surface fault ruptures extends straight except for the damages on the fault traces. House damages along the surface fault ruptures with normal slip were rather small suggesting that ground shaking was not so strong.

Keywords: Kumamoto earthquake, fault geometry, house damage

# Real-time Damage Estimations for the 2016 Kumamoto Earthquakes by J-RISQ

\*Hiromitsu Nakamura<sup>1</sup>, Hiroyuki Fujiwara<sup>1</sup>, Ikuo Takahashi<sup>1</sup>, Naokazu Momma<sup>1</sup>, Yoshinori Homma<sup>2</sup>

1. National Research Institute for Earth Science and Disaster Prevention, 2. Mitsubishi Space Software

The National Research Institute for Earth Science and Disaster Resilience (NIED) is developing a real-time earthquake information system for damage estimation and situation assessment (J-RISQ) as a Cross-ministerial Strategic Innovation Promotion Program (SIP). J-RISQ is able to immediately estimate earthquake damage by combining methods for predicting ground motion using amplification characteristic data for subsurface ground, basic information on population and buildings, damage assessment methods for buildings using fragility functions, and observation data such as real-time strong motion data obtained by K-NET, KiK-net, local governments, and JMA. A part of J-RISQ information is published as a "J-RISQ Report" on <http://www.j-risq.bosai.go.jp/> immediately after the occurrence of an earthquake. In this study, we describe the estimations by J-RISQ for the 2016 Kumamoto earthquakes (M6.5 event and M7.3 event) with maximum seismic intensity of 7 caused great damage to human beings, buildings, and infrastructures.

J-RISQ issued the first report 29 seconds after the M6.5 event occurred and a total of seven reports for about 10 minutes. Finally the system estimated that population exposed to seismic intensity of 6 lower or larger was 620,000 and that of 6 higher or larger was 290,000. The estimated results of building damage showed that completely destroyed buildings were between 6,000 and 14,000. The distribution of estimated completely destroyed buildings spread 7 km long by 1 km wide in Mashiki town.

For the M7.3 event occurred about 28 hours after the M6.5 event, the system distributed the first report 29 seconds after the M7.3 event occurred and a total of eight reports for about 11 minutes. Finally the system estimated that population exposed to seismic intensity of 6 lower or larger was 1,130,000 and that of 6 higher or larger was 660,000. The estimated results of building damage showed that completely destroyed buildings were between 12,000 and 31,000. The distribution of estimated completely destroyed buildings spread in Mashiki town similar to the result of the M6.5 event and Kumamoto city. However, this result of damage building is out of consideration of the effect of the earthquakes including M6.5 event before M7.3 event.

The estimated spatial distribution of the belt-shaped region at Mashiki town qualitatively agrees with the actual damage status; however, the estimated results tend to overestimate the actual damage. Therefore, we aim to verify the precision of the estimated damage through a detailed investigation of damage to buildings and to make improvements to enhance precision. Building damage caused by the Kumamoto earthquakes may be attributed to the decreased strength of buildings because of repeated strong motion originating from the large foreshock, mainshock, and subsequent active seismic activity. We also plan to investigate real-time damage estimation methods taking into account such changes in building strength.

## Acknowledgements

This work was supported by the Council for Science, Technology and Innovation (CSTI) through the Cross-ministerial Strategic Innovation Promotion Program (SIP), titled "Enhancement of societal resiliency against natural disasters" (Funding agency: JST). The seismic intensity data from local governments and JMA that were used in the real-time system were provided by JMA.

Keywords: Kumamoto earthquake, Real-time Damage Estimation, J-RISQ

## Modeling of the subsurface structure from the seismic bedrock to the ground surface for a broadband strong motion evaluation during 2016 Kumamoto earthquake.

\*Shigeki Senna<sup>1</sup>, Kaoru Jin<sup>1</sup>, Atsushi Wakai<sup>1</sup>, Hiroki Azuma<sup>1</sup>, Shohei Naito<sup>1</sup>, Nobuyuki Morikawa<sup>1</sup>, Takahiro Maeda<sup>1</sup>, Asako Iwaki<sup>1</sup>, Ryuji Yamada<sup>1</sup>, Shinichi Kawai<sup>1</sup>, Hisanori Matsuyama<sup>2</sup>, Hiroyuki Fujiwara<sup>1</sup>

1. National Research Institute for Earth Science and Disaster Prevention, 2. OYO Corp

On April 16, 2016, a Japan Meteorological Agency Magnitude (MJMA) 7.3 earthquake struck the Kumamoto Prefecture on the island of Kyushu in southwest Japan. This earthquake followed the MJMA 6.5 earthquake, which struck on April 14. Both the earthquakes registered a reading of 7 on the Japan Meteorological Agency seismic intensity scale (IJMA), which is the highest reading on the IJMA, in the town of Mashiki approximately 6.5 and 5.5 km from the hypocenters of the main shock and foreshock, respectively.

The tendency damage is concentrating at the earthquake fault neighborhood confirmed the building damage distribution. However, even if damage is away from a little location and the fault even if it's right above the gap, the location where damage is big relatively is also confirmed. There is also comment with a high possibility caused by soil structure for these phenomena. We put it around Kumamoto plain in the fault neighborhood, collected borehole data and built initial stage geologic model, and a microtremor observation and seismography record were collected.

And secondary S-wave velocity model built highly precise ground model and did comparison and consideration with the building damage distribution.

This research was conducted by SIP (Cross-ministerial Strategic Innovation Promotion Program), "reinforcement of resilient disaster prevention and mitigation function" of Council for Science, Technology and innovation.

Keywords: Strong motion evaluation, S-wave velocity structure model, Microtremor array, Borehole data, Predominant period

# Relationship between active fault landform and surface rupture accompanied with 2016 Kumamoto Earthquake

\*Yasuhiro Kumahara<sup>1</sup>

1. Graduate School of Education, Hiroshima University

On 16 April 2016, a  $M_w=7.0$  ( $M_{jma}=7.3$ ) earthquake hit from Kumamoto city to the Aso volcanic Caldera in central Kumamoto Prefecture, central Kyushu. Prior to the 16 April earthquake, the 14 April  $M_w=6.2$  ( $M_{jma}=6.5$ ) earthquake was also generated at close to the epicenter of the 16 April Earthquake in east of Kumamoto City. It is well known that there is a north part of the Futagawa-Hinagu fault system (FHFS), mapped by previous studies (e.g. Research group for active tectonics in Kyushu ed, 1989; Nakata and Imaizumi ed, 2002) in the epicentral area. The photo-interpretation method is common to map the fault trace in Japan. Because the traces of the FHFS run below the dense forest and village, the cumulative offset along the FHFS was not mapped sufficiently. The 2 m-grid Digital Elevation Model along the FHFS acquired by the GSI provided us the firm evidences of cumulative right-lateral strike-slip along the FHFS, and also Idenokuchi fault, parallel to the Futagawa fault. Here we show the relationship between tectonic landform and surface rupture accompanied with Kumamoto Earthquake.

Keywords: Kumamoto Earthquake, Surface rupture, Active fault



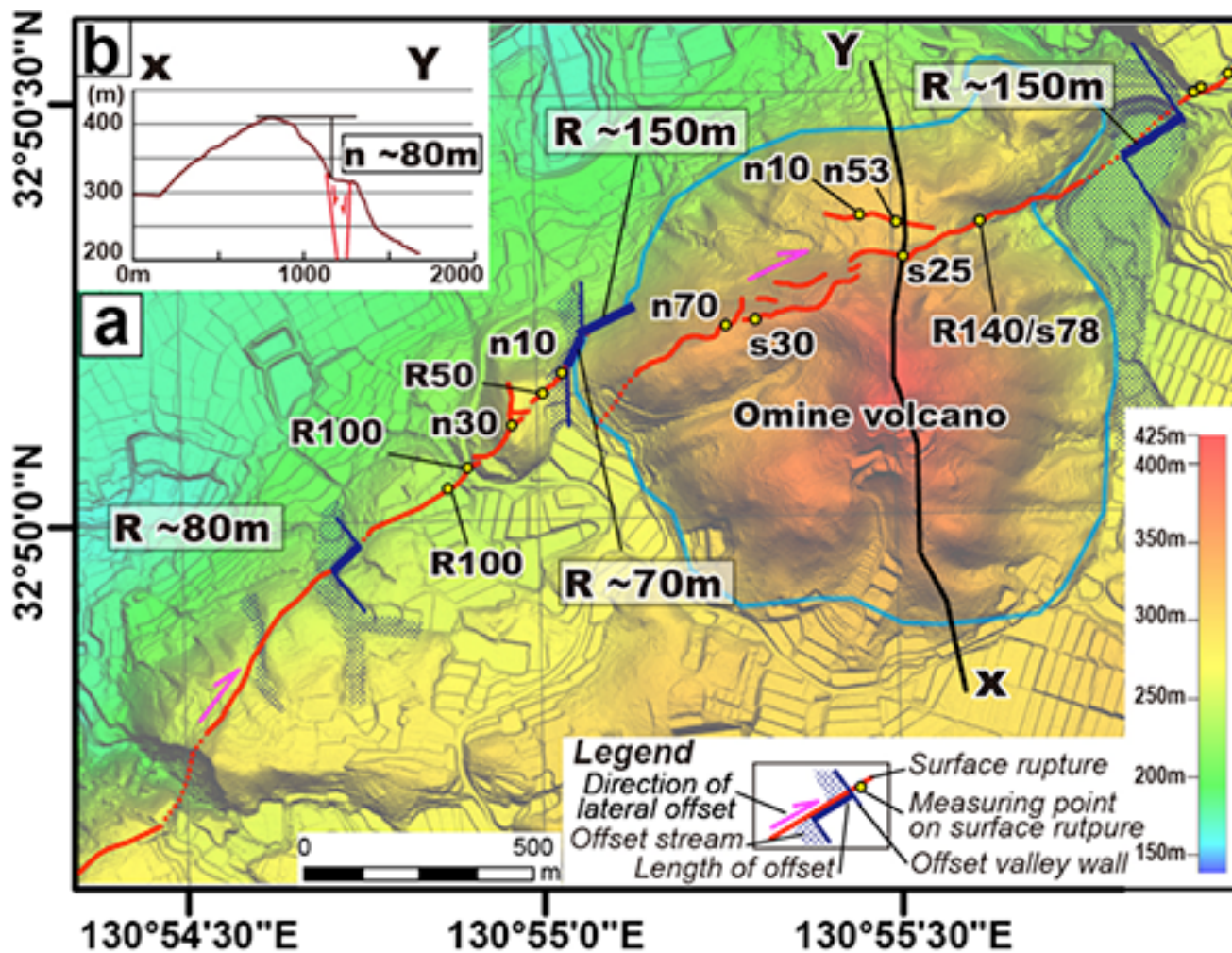


Figure 1 surface rupture with displacement and cumulative offset on the rupture in Oomine, Nishihara.

# Utilizing 8K Super Hi-Vision for Disaster Mitigation and Geosciences: reporting from the 2016 Kumamoto earthquake in Japan

\*MASARU YAMAGUCHI<sup>1</sup>

1. NHK Japan Broadcasting Corporation, Broadcasting Culture Research Institute

NHK (Japan Broadcasting Corporation) launched test broadcasting of 4K/8K(super hi-vision) in 2016. This presentation clarifies the fact that 8K, ultra-high definition image, 16 times that of HDTV(2K), is useful for not only broadcasting but also disaster research and geosciences in terms of remote sensing, space information.


NHK used an 8K small camera in aerial filming of areas along active faults that were severely damaged immediately after the 2016 Kumamoto earthquake. As we had active fault scientists analyze the footage, undiscovered earthquake faults and ruptures were found, which were reported in an NHK's TV program. This served as the first utilization of disaster analyses of 8K images in disaster reporting in media.

Aerial filming using an 8K camera enables discovery of ruptures as small as a few centimeters from an altitude of 400 meters, and provides "higher resolution" than aerial photography and "wider angles of view" than 4K drones. Since ruptures may cause a variety of disasters, there are high expectations for the utilization of 8K images in DRR. 8K images also allow the observation of each individual's "move," which will be effective for life-saving and search operations and detecting temporary shelters. 8K's "oblique bird's-eye views" provides vertical information that will make it easier to survey collapsed buildings, and its graphics data can be utilized for making "3D models" and "crisis maps."

Reference: Yamaguchi(2017) Possibility of Utilizing 8K Super Hi-Vision for Disaster Risk Reduction The NHK Monthly Report on Broadcast Research (Japanese)

<http://www.nhk.or.jp/bunken/english/reports/summary/201701/01.html>

Keywords: active fault, 8K Super Hi-Vision, remote sensing, Media, Japan broadcasting corporation, disaster

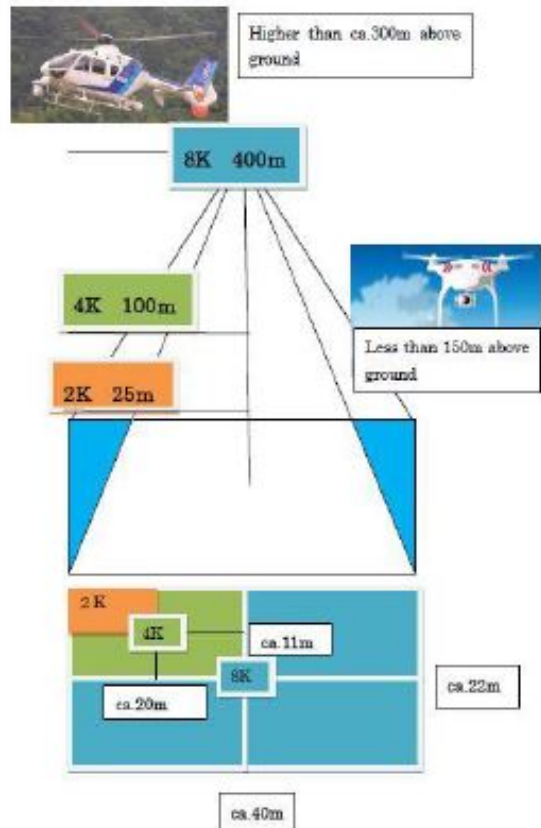


HDTV(2K)      4K      8K Super Hi-Vision

The 8K Super Hi-Vision system supports higher frame rates to enable vivid reproduction of the subject, in addition to ultra-high definition video of approximately 33 megapixels. Also, the wider color gamut and greater bit depth have made it an ultimate TV broadcasting system capable of reproducing bright colors more accurately.

### 8K Super Hi-Vision image

Aspect ratio	16 : 9
Pixel number	7,680 × 4,320
Frame rate	120, 119.88, 60, 59.94 Hz Progressive
Scanning	Progressive
Bit depth	10, 12 bit
Color gamut	Wide gamut system colorimetry



**resolution:** The ground pixel size  
**5 mm :** 8K (this study)  
**100 mm :** aerial photograph of Geospatial Information Authority of Japan

**You can watch flying butterfly on the ground shot by 8K camera from 400m high above ground.**

# Estimation of Slip Velocity Function for the Region Shallower than Seismogenic Layer

\*Tanaka Shinya<sup>1</sup>, Kazuhito Hikima<sup>2</sup>, Yoshiaki Hisada<sup>3</sup>

1. Tokyo Electric Power Services Co., Ltd., 2. Tokyo Electric Power Company, 3. Kogakuin University

## 1. Introduction

The 2016 Kumamoto earthquake (Mw7.0) generated the expensive surface faulting, and recorded characteristic near-fault strong motions. For this reason the main attention has been directed to estimation of near-fault strong ground motion and the fling step. The theoretical method is widely used for estimation of near-fault strong ground motion, but little is known about slip velocity function required for estimation, especially the region shallower than seismogenic layer. According to Hikima et al. (2015), slip velocity function in the shallow section of the faulting area are different from that in the deep section. The purpose of this study is to estimate slip velocity function for the region shallower than seismogenic layer using near-fault strong ground motions and source fault models.

## 2. Study on the 1999 Chi-Chi Earthquake

The 1999 Chi-Chi earthquake (Mw7.6) recorded near-fault strong ground motions. TCU068, TCU102 are lying on the hanging wall, and TCU052 is lying on the foot wall. We simulated these observation records by theoretical method. Figure 1 shows slip velocity function identified by Wu et al. (2001) close to strong-motion stations. Figure 2 shows comparison of synthetic and observation waveforms fittings. Figure 2 include three sets of synthetic waves; the top waves (case1) simulated using source fault model by Wu et al.(2001). The middle waves (case2) correspond to simulated using only subfaults close to strong-motion stations, about 10km long and 6km wide. The bottom waves (case3) correspond to simulated using subfaults close to strong-motion stations similarly case2. In addition, we used average slip of subfaults close to strong-motion stations and a simple triangle time window as slip velocity function. For TCU068 and TCU102 lying on the hanging wall, the synthetic waves of case1 and case2 are in good agreement with observation records. Subfaults close to strong-motion stations dominates in velocity and displacement waveforms. In addition, observation velocity waveforms are very similar to slip velocity function of subfaults close to strong-motion stations. Since we approximate slip velocity function as a simple triangle time window (that is case3). We estimated that the values for duration of triangle time window as slip velocity function and average slip of subfaults close to TCU068 were 5sec and 8.2m, TCU052 were 7sec and 12.1m, respectively. As a result, the synthetic waves of case3 are in good agreement with observation records.

Whereas, observation velocity waveforms of TCU052 lying on the foot wall has a different from slip velocity function. In addition, it cannot be said that subfaults close to strong-motion stations dominates in velocity waveforms. One reason for this is the greater are that displacement on the footwall is smaller than on the hanging wall because of low dip angle (about 30°). It was noted that it is difficult to approximate slip velocity function from only near-fault strong ground motions. Besides, it may be suspected that accuracy of slip velocity function is low if strong-motion stations lie only on the foot wall of low-angle fault. Incidentally, we estimated that the values for duration of triangle time window as slip velocity function and average slip of subfaults close to TCU102 were 6sec and 9.6m, respectively.

## 3. Estimation of Slip Velocity Function

In light of these considerations we estimated slip velocity function for the region shallower than seismogenic layer for other earthquakes in the same way as 1999 Chi-Chi earthquake. It was found that

the duration of triangle time window as slip velocity function correlates positively with average slip of subfaults close to strong-motion stations as shown in Fig.3. Further studies for more earthquakes are needed in order to improve the accuracy of estimation of near-fault strong ground motion.

Acknowledgments: The source fault model for this work was provided by Dr. Wu. The authors wish to thank him.

Keywords: Near source region, Slip velocity function, the Seismic Waveform Inversion, Strong ground motion prediction

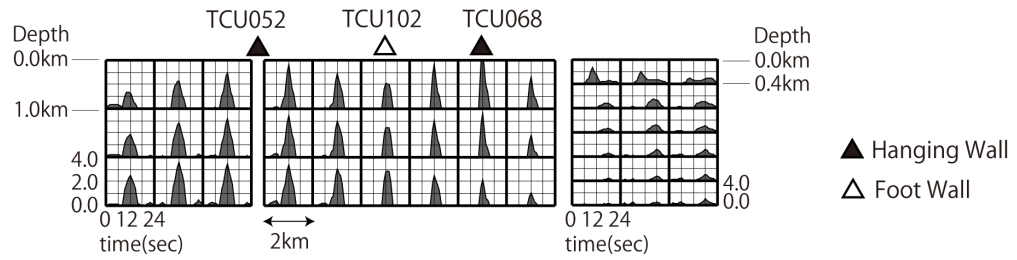


Figure 1. Slip velocity function by Wu et al.(2001) near strong-motion stations in the northern part of 1999Chi-Chi

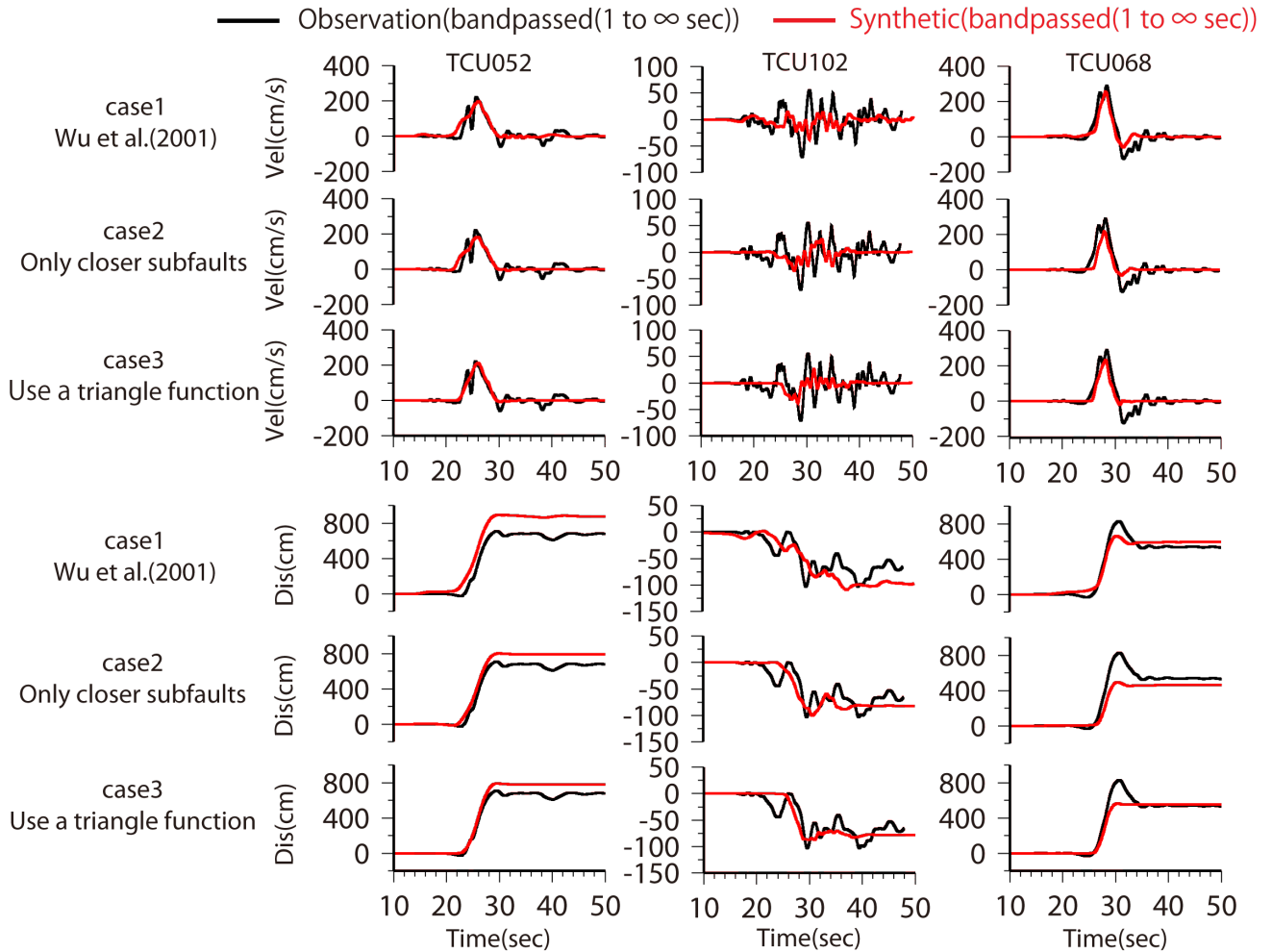


Figure 2. Comparison of synthetic and observation waveform fittings ( NS component, 1999Chi-Chi )

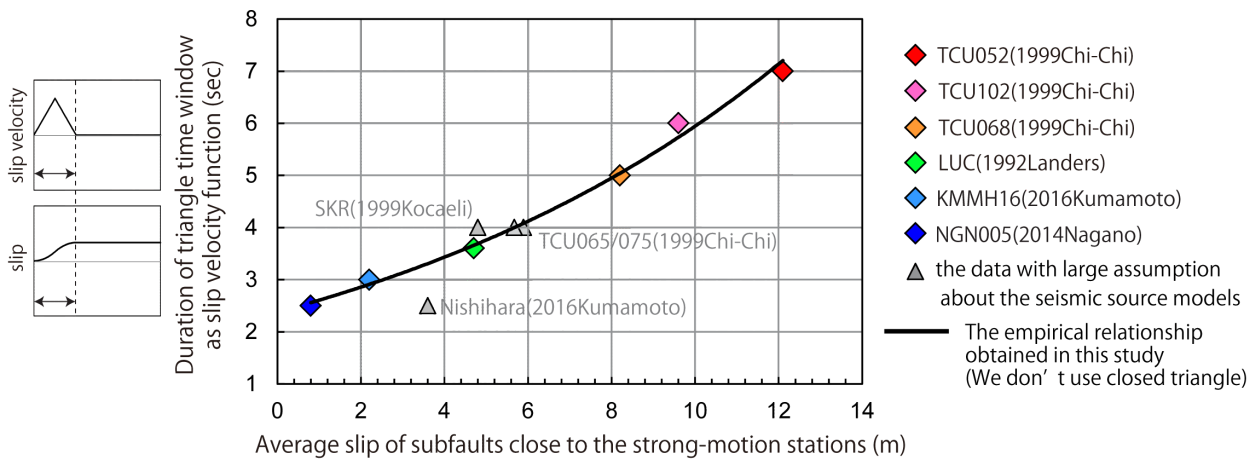


Figure 3. Relationships among slip velocity function and slip in shallower region than the seismogenic layer

# A study on modeling method of active faults with surface rupture for strong ground motion evaluation

\*Nobuyuki Morikawa<sup>1</sup>, Hiroyuki Fujiwara<sup>1</sup>, Asako Iwaki<sup>1</sup>, Takahiro Maeda<sup>1</sup>

1. National Research Institute for Earth Science and Disaster Resilience

In the strong-motion evaluation, the emphasis was mainly on modeling of short period strong-motion generation, the source faults was within the seismogenic layer, and its upper end was not 0km (surface). However, it is necessary to model the upper end of the source fault at 0km up even in strong-motion evaluation for earthquakes occurring in active faults where clear surface fault is identified.

As a first step to extend the source fault model to the ground surface in strong-motion evaluation, here we considered three models for the main shock of the 2016 Kumamoto earthquake (Mw=7.0) as below;

Model-1: The upper end and width of the source fault are 0km and 18km,

Model-2: The upper end and width of the source fault are 2km and 18km,

Model-3: The upper end and width of the source fault are 2km and 16km.

We assumed that the length of the source fault was 34km, which was same as the length of recognized surface fault, and seismic moment was  $4.5 \times 10^{19}$  Nm in all models. And we applied the strike and dip as same as the model for the Futagawa segment of Futagawa fault zone by Headquarters for Earthquake Research Promotion (2014). Source parameters. For model-1, we set up two types of models. The one was using slip velocity time functions by Nakamura and Miyatake (2000) for whole source fault (Model-1NM). The other was using smoothed ramp type slip time functions for shallower than the top of the seismogenic zone (2km; Model-1SR). The locations of hypocenter and asperities were common to all models.

We performed strong-motion simulations for the above four source models using a 3-D underground velocity structure model J-SHIS V2 (Fujiwara et al., 2012). The main results are follows.

1. The difference of strong-motion distribution between Model-1 and others can be seen at region where distance from surface fault is within 2km.
2. There is almost no difference in strong-motion distribution at region where distance from surface fault is farther than 2km.
3. In Model-1NM, a abnormal waveform appears at some sites. It causes extremely large PGV and/or JMA seismic intensity.

We conclude that strong-motion evaluation for earthquakes in active faults whose the upper end of the source fault is 0km by using a smoothed ramp type slip time function for shallower than the seismogenic zone can provide appropriate results comparable to previous evaluations. However, it is necessary to establish a detailed modeling method of the position and shape of the source fault, the slip velocity time function at shallower part of the source fault.

Keywords: The 2016 Kumamoto earthquake, surface fault, strong-motion evaluation

## Ground motion amplification obtained with microtremor, aftershock and borehole measurements in heavily damaged zone in the Mashiki town, Kumamoto prefecture

\*Masayuki Yoshimi<sup>1</sup>, Hiroyuki Goto<sup>2</sup>, Yoshiya Hata<sup>3</sup>, Yoshikazu Shingaki<sup>4</sup>, Takashi Hosoya<sup>5</sup>, Sachiko Morita<sup>5</sup>, Takeshi Sugiyama<sup>6</sup>, Tetsuyoshi Tokumaru<sup>6</sup>

1. Geological Survey of Japan, AIST, 2. DPRI, Kyoto University, 3. Osaka University, 4. TEPSCO, 5. Chuo-Kaihatu Corporation, 6. Tokumaru PE office

Heavily damaged zone by the ground motion of the 2016 Kumamoto earthquake, Japan, was recognized in the downtown area of the Mashiki town, Kumamoto prefecture. Five records of the mainshock in/around the zone show that the ground motion in the zone were about 2-3 times stronger than that observed at KMMH16 in terms of the linear response around the period 1 sec. (Hata et al., 2016), which might explain difference of the damage. Goto et al. (2016, 2017) demonstrated that the nonlinear response of the shallower soil (down to 50 m as much) owed much to the amplification. We conducted borehole survey (Yoshimi et al., 2016, 2017; Shingaki et al., 2017), aftershock and microtremor observation at three sites in the damaged zone. Site amplification characteristics of those sites in linear and nonlinear regime will be demonstrated.

Keywords: 2016 Kumamoto Earthquake, Ground amplification, Aftershock observation, Borehole survey, nonlinear site response



## Relationship between subsurface structure and large-scale fissures in the northwestern region in Aso valley caused by the 2016 Kumamoto earthquake

\*Issei Doi<sup>1</sup>, Toshitaka Kamai<sup>1</sup>, Satoshi Goto<sup>2</sup>, Ryohei Azuma<sup>3</sup>, Takahiro Ohkura<sup>4</sup>, Hidehiko Murao<sup>5</sup>, Kenji Mima<sup>6</sup>

1. Disaster Prevention Research Institute, 2. Integrated Graduate School of Medicine, Engineering, and Agricultural Sciences, Yamanashi University, 3. Faculty of Engineering, Osaka Institute of Technology, 4. Graduate School of Science, Kyoto University, 5. Murao Chiken, 6. Ohta Geo Research. Co., Ltd.

In accompanied with the 2016 Kumamoto earthquake, fissures with the length and the height a few hundred meters and two meters, respectively, emerged in Aso valley (inside the Aso caldera). In this area, the top layer consists of sediments in the caldera lake created by Aso-4 eruption with the thickness a few tens of meters. InSAR and seismic data show that the region with the size of 1-4 square meter moved 1-2 m northward horizontally during strong motion of the mainshock (Fujiwara et al., 2016; Doi et al., 2016). We investigated the mechanism of the movement of these regions by estimating subsurface structure beneath this area.

Two station spatial auto-correlation (2ST-SPAC) method (Hayashi and Craig, 2016) was applied to estimate subsurface structure using ambient noises. We succeeded to estimate the S-wave velocity structure to the depth of 130 m in and around the regions with fissures. In the regions where large scale fissures were developed, a layer with S-wave velocity less than 150 m/s lay from the surface to the depth of 60 m, followed by two layers with 250 m/s and 300 m/s at depths of 60-90 m and 90-130 m, respectively. This low-velocity layer was considered to represent soft sediments in the caldera lake due to Aso-4 eruption and consistent with the nearby boring profile. Two relatively higher layers might correspond to lava layers after Aso-4 eruption. Moreover, the S-wave velocity at the top surface to the depth of 5 m was so slow as 80 m/s. We continue to estimate the distribution of the soft sediments and lava structure beneath them, to elucidate how fissures were generated in this area.

# The characteristics of damaged buildings due to the 2016 Kumamoto Earthquake in Mashiki town

\*Takahito Kuroki<sup>1</sup>, Nozomi Iso<sup>2</sup>

1. Faculty of Education, Univ. of Teacher Edu. Fukuoka, 2. Department of Human Sciences, Seinan Gakuin University

The 2016 Kumamoto Earthquake caused huge damages to many buildings and infrastructures in Kumamoto city, Mashiki town and others inside of the area in Kumamoto plain, central Kyushu. These damages occurred along two active fault zones, Futagawa fault zone and Hinagu fault zone. Many faults or co-seismic surface ruptures appeared to large damages on many buildings in central Mashiki town, because this area situated a cross zone on the extended part of the two fault zone. This study reports some characters of damaged buildings which were obtained by the observation of more than 3,600 buildings in 1.43 km<sup>2</sup> of central Mashiki and reports some characters of more than 330 co-seismic surface ruptures occurred there.

We checked 6 items of each building character in the study area. They are damage degree, type of building use, building age, roofing material, building material and tilted building direction. The damage degree of buildings was classified to 5 sections, counted large damaged 409, middle damaged 464, small damaged 575, covered roof 349 and no damaged 1,427. The type of building use was separated to 3 sections, counted residence 2,456 buildings, warehouse 770 buildings and nothing or removed 352 buildings. The building age was classified to 4 sections, counted very old 118 buildings, old 1,652 buildings, new 1,172 buildings and very new 281 buildings. The roofing material was separated to 3 sections, counted ceramic tile 1,472 buildings, slate one 706 buildings and other 1,045 buildings. The building material was divided to 2 sections, counted combustibleness 2,439 buildings and incombustibleness 813 buildings. The tilted building direction was measured, counted the north direction 232 buildings, the east direction 374 buildings, the south direction 442 buildings and the west direction 442 buildings.

We calculated the percentage of degree of damage for each item, and then we found the characters of damaged buildings as follows. From the building use type analysis, we found the damage ratio of residence was higher than that of warehouse. From the roofing material analysis, we found the damage ratio of ceramic tile was higher than that of slate one or other. From the building material analysis, we found the damage ratio of combustibleness is higher than that of incombustibleness. From the tilted building direction analysis, we found majority of the direction was the east-west which showed close direction to the strike of the earthquake faults. From the damage degree analysis, we found the damage ratio was high when the building was old and the ratio was low when the building was new. In other words, the degree of building damage levels was lower when the building was new.

From these analyses, we reclassified damage degree of building into 5 degrees from 1 to 5, arranged from easy to heavy. Distributional map of the damage degree was made by using a spatial-filtering GIS function. Therefore the severely damaged zone was indicated clearly in this area. It is important that earthquake surface faults and/or co-seismic surface ruptures concentrated at the marginal area of this zone.

Keywords: the 2016 Kumamoto Earthquake, damaged building, earthquake fault, GIS

# Spatial distribution analysis of buildings with middle-level damage following Kumamoto earthquakes in 2016

\*Hiroto Nagai<sup>1</sup>, Ryo Natsuaki<sup>1</sup>

1. Japan Aerospace Exploration Agency

A series of M6-7 class earthquakes were initiated on April 14, 2016 around Kumamoto. Following these events, many buildings were covered with plastic sheets to facilitate repair, making their spatial distribution heterogeneous. By assuming this spatial heterogeneity of building damage, this study clarifies the spatial distribution of buildings. In addition, relationships with geomorphological factors are considered, and a preliminary method for early recognition of damage distribution using a remote sensing technique is determined.

Google Earth is a well-known digital earth software used globally. In this study, three-dimensional post-quake building models located around Kumamoto city taken by aerial photography a few weeks after the quakes were identified from Google Earth. The images enabled viewing from all angles; roofs with plastic sheets were visually identified, mostly as blue, green, and white, and their locations were recorded and defined as "middle-damaged building (MDB)". Such buildings were the ordinal residences of individual families and also commercial multiple-floor buildings. Multiple sheets on a single building were regarded as one MDB. Green houses on farms, exterior objects, vehicles, and buildings under construction were excluded from analysis. In addition, digitized information of the original and whole building distribution was obtained from the Geospatial Information Authority of Japan (GSI) (i.e. two-dimensional polygons of building outlines).

Geospatial statistics show 15675 MDBs out of a total of 165177 buildings (9.5%). Spatial distribution on a GSI geomorphologic map shows that all buildings are mainly distributed as follows: 40.2% on terrace, 14.8% on alluvial fan, 15.0% on flood plain, and 8.0% on natural levee; whereas the distribution of MDBs is as follows: 13.0% on terrace, 5.5% on alluvial fan, 5.3% on flood plain, and 6.7% on natural levee. These results suggest that buildings on a terrace have are relatively more likely to suffer damage compared to those on an alluvial fan, flood plain, or natural levee. Although catastrophic devastation is significantly identified near the moved active fault (e.g. Mashiki town in Kumamoto), the occurrence of moderate damage (where buildings could possibly be reused after repair) has a remarkable correlation with geomorphologic condition type. Further discussion is expected in relation to characteristics of the earthquake mechanism.

Significant surface change causes a decrease in coherence in the interferometric processing of synthetic aperture radar, and there is thus less similarity between the reflected phases. This method is used to determine the distribution of damaged buildings. Normalized coherence decrease (NCD) is calculated using PALSAR-2 data observed on November 30, 2015, March 7, 2016 (both for pre-quake), and on April 18, 2016 (post-quake). The frequency of NCD values on MDBs and those for whole buildings show statistically different distributions within histograms. This result shows that moderate damage occurring to the roofs of buildings causes a higher NCD. Further improvement is thus required to detect individual damaged buildings in a case of hazard response.

Keywords: Remote sensing, ALOS-2, Geomorphology, Coherence

# The running photographic investigation by an automobile for estimating building damages of 2016 Kumamoto earthquakes

\*Shohei Naito<sup>1</sup>, Hiromitsu Nakamura<sup>1</sup>, Hiroyuki Fujiwara<sup>1</sup>

1. National Research Institute for Earth Science and Disaster Resiliense

It is crucial to develop methods for get a prompt overview of the damage situation soon after the earthquake, in terms of supporting decision-makings quickly. For this reason, we have been developing the Japan real-time information systems for earthquake (J-RISQ).

Both in cases of the foreshock (M6.5) on April 14 and the main shock (M7.3) on April 16, J-RISQ have published final reports of 2016 Kumamoto earthquakes which includes estimated distributions per 250-meter meshes of seismic intensities, exposed populations, and building damages, approximately within 10 minutes. These estimations indicate a belt of destructive area adjacent to Mashiki town, and also correspond approximately to actual damaged area. However, it still have several problems like estimated results of building damages were overestimated, and it have not been considerable for sequential shakings of aftershocks.

To verify and improve the real-time damage estimation methods, we have to gather information of the actual damage caused by 2016 Kumamoto earthquakes by multiple ways such as field investigations, aerial photographs, running investigations by automobiles.

In this paper, we are going to describe about the running photographic investigation by an automobile. We have performed running surveys from April 17<sup>th</sup> to 28<sup>th</sup>, in Kumamoto city, Nishihara village, Mifune town, Kashima town, Mashiki town, and Kousa town. The total running distances are 576 km.

We have acquired digital images every 5 meters with 6 cameras installed inside the automobile, additionally, the location and time of these cameras are synchronized with GPS. Then, we have extracted the 7,584 photographs of buildings from 571,700 photos. In the next place, we have chosen 593 total collapsed buildings by the standard of classification chart of the building damage released by Cabinet Office.

As a result, the distribution of total collapsed buildings are within the rage of 1 km around surface ruptures caused by 2016 Kumamoto earthquakes. These distribution is also coordinate with the damage concentrate area estimated by field investigations and aerial photographs.

From now on, we are going to develop methods for estimating building damages by way of the machine learning with extracted damage photographs. These methods would be actualize more detail and immediate damage estimation.

Acknowledgment:

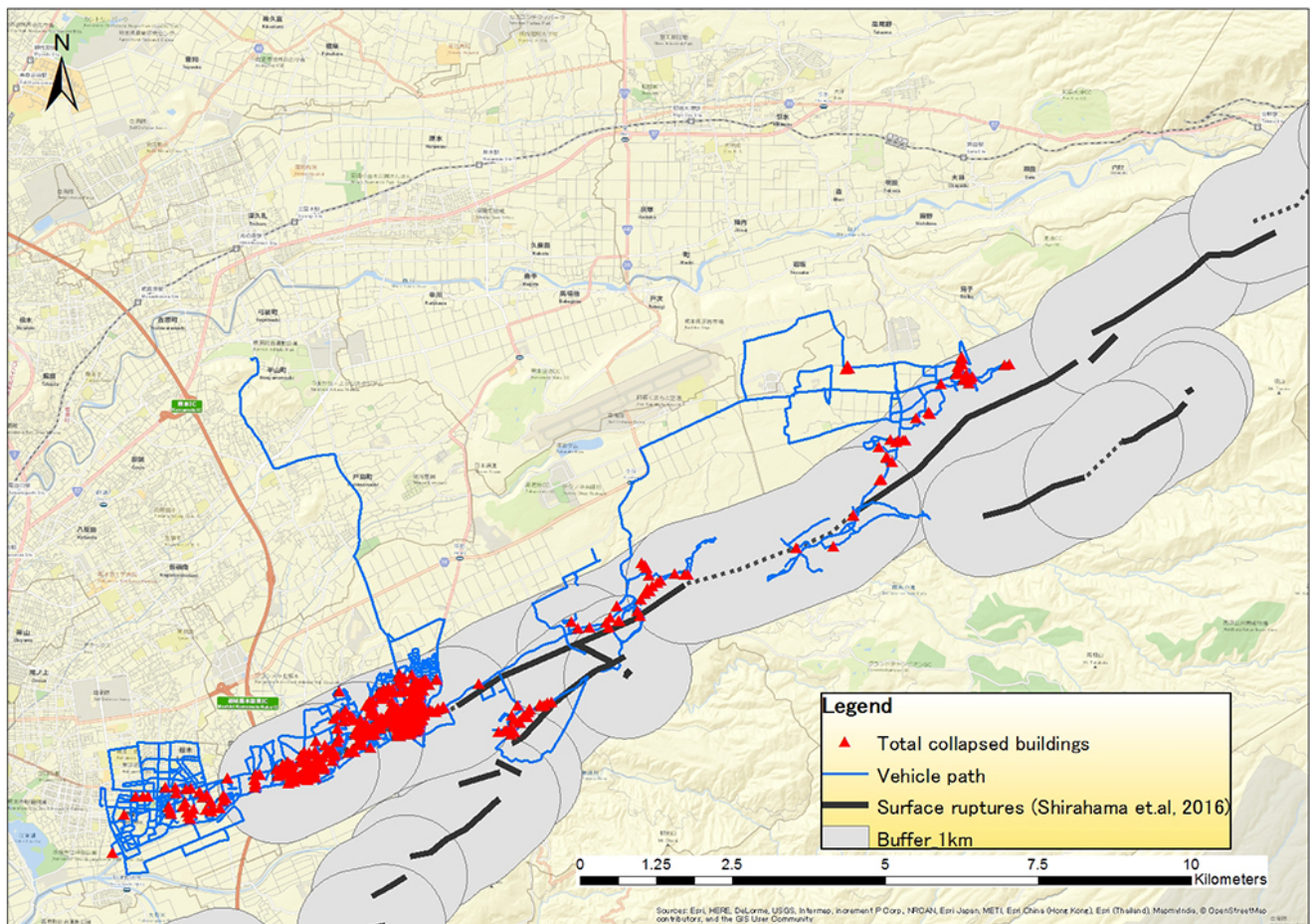
This work was (partially) supported by the Council for Science Technology and Innovation (CSTI) through the Cross-ministerial Strategic Innovation Promotion Program (SIP), titled “Enhancement of societal resiliency against natural disasters” (Funding agency: JST).

References:

H.Nakamura, H.Fujiwara, T.Kunugi, S.Aoi, S.Senna, I.Takahashi, S.Naito, and H.Azuma: Development of real-time earthquake damage information system in Japan, 16th World Conference on Earthquake, Santiago Chile, 2017.

Y. Shirahama, M.Yoshimi, Y.Awata, T.Maruyama, T.Azuma, Y.Miyashita, H. Mori, K.Imanishi, N.Takeda, T.Ochi, M.Otsubo, D.Asahina, and A.Miyakawa, “Characteristics of the surface ruptures associated with the 2016 Kumamoto earthquake sequence, central Kyushu, Japan” , Earth Planets and Space(2016), 68:191.

Keywords: Kumamoto earthquake, Building damage, Running investigation, Photographic interpretation, Active fault



## Feature of the building damage of Kumamoto earthquake by airphoto-interpretation

\*naokazu momma<sup>1</sup>, hiroyuki fujiwara<sup>2</sup>, hiromistu nakamura<sup>2</sup>, takuma saeki<sup>2</sup>, hiroyuki shimomura<sup>1</sup>, tetuya yamada<sup>1</sup>, seiiji fujisawa<sup>1</sup>

1. PASCO Co, 2. National Research institute for Earth science and Disaster resilience

In Kumamoto-ken, an earthquake of magnitude 6.5 (fore-shock) occurred on April 14, 2016 and an earthquake of magnitude 7.3 (main shock) occurred on April 16. Mashiki-machi and Nishihara-mura recorded seismic intensity 7 by this earthquake, and enormous building damage occurred. We investigated building damage targeted for Mashiki-machi, Nishihara-mura, Kumamoto-shi, Uto-shi, Uki-shi, Aso-shi, Kashima-machi, Kosa-machi, Ozu-machi and the minami Aso mura. Investigation method is the way by which watch reads building damage from the air photo taken a picture of after fore-shock and main shock. The large (collapse and tear), the medium (partial destruction) and the small (part damage) and without divided the degree of the damage into reading of building damage. When the distribution of the building of the damage large by the main shock is seen, the damage large is distributed over the northeast-southwest direction successively from the south Aso village to Kumamoto-shi Higashi-ku. Mashiki-machi excels with about 1,400 houses, and have a lot of number of houses of the damage large. Nishihara-mura, Kumamoto-shi Higashi-ku, Kashima-machi and the south Aso village are 150-180 houses. In Mashiki Town, the about 85% number of damage large is estimated by seismic intensity 7, the remaining is seismic intensity 6 strong. We calculated the collapse rate of the damage size of 250 m mesh. Looking at the relationship with constant seismic intensity, the collapse rate tends to increase as the estimated seismic intensity increases. However, even with the same seismic intensity value, the collapse rate has the largest width to the minimum and maximum.

Keywords: Kumamoto earthquake, airphoto-interpretation, building damage, seismic intensity, collapse rate

## Relationship between building damage and liquefaction sites during the 2016 Kumamoto Earthquake

\*Ozawa Kyoko<sup>1</sup>, Shigeki Senna<sup>1</sup>, Hiroyuki Fujiwara<sup>1</sup>

1. National Research Institute for Earth Science and Disaster Prevention

During the 2016 Kumamoto Earthquake that occurred on April 14 and 16, 2016, liquefaction occurred over the large area. We checked a relation between a liquefaction sites and building damage levels in this study.

We judged liquefaction sites at the mesh size of 50m using high-resolution aerial photographs, and found liquefaction for about 5,800 meshes. Comparing this result with building damage data, we checked a relation between them.

It seems that building damage is heavier at liquefaction sites in Kumamoto city. This indicates that liquefaction can affect building damage levels also in other areas.

Liquefaction was caused over the large area due to the Kumamoto earthquake. We checked a relation between liquefaction sites and building damage levels based on each investigated results. Then, it was found that building damage tended to be heavier due to liquefaction in a certain area. It is necessary to investigate the relation in more details using other types of liquefaction data from now on.

Keywords: the 2016 Kumamoto Earthquake, liquefaction, building damage

# Simulation of building damage distribution by the 2016 Kumamoto Earthquake by use of limited information on real damage

\*Akihiro Kusaka<sup>1,2</sup>, Hiromitsu Nakamura<sup>1</sup>, Hiroyuki Fujiwara<sup>1</sup>, Katsuhisa Kanda<sup>2</sup>, Naokazu Momma<sup>1</sup>

1. National Research Institute for Earthquake Science and Disaster Resilience, 2. Kobori Research Complex Inc.

## 1. Introduction

In case of widely spread disaster such as a great earthquake, a disaster information system is under development to gather and estimate the whole damage situation in “real-time” in order to support decision-making for initial corresponding. In a very short time after an earthquake occurs, the system estimates ground motion distribution by each 250m regional mesh by interpolating strong motion records which are gathered by nationwide observation station networks, K-NET and KiK-net etc. Then, it combines the estimated ground motion distribution with prepared fragility functions and exposure data to estimate the number of damaged houses. Moreover, a method to improve the estimated accuracy is being developed, by use of actual damage information on limited areas as “observation” in Bayesian updating protocol. This report deals with numerical examples of the method.

## 2. Updating framework for estimation error in numbers of damaged houses

The system, at first, generates “immediate estimates” which is based on ground motion distribution and prepared fragilities and exposure data. In the estimation, errors of the parameters of fragilities are modeled as random variables. Then, the parameters of probability distributions are updated by Bayesian protocol by use of actual damage information such as the real numbers of damaged houses in some particular areas.

## 3. Actual damage information read from aerial photographs

This study uses the numbers of damaged houses in each 250 m mesh as actual damage information. They are read by eyes from the oblique photographs took from a helicopter after occurrence of the Earthquake (Mw 7.3) on April 16th.

In the numerical examples, we use only a part of information; that on some selected meshes, in order to examine how to improve the estimation accuracy even with as small data as possible. The selecting process is as followings: 1. Chose meshes those include twenty or more houses from some districts, where are determined with reference to the estimated ground motion distribution. 2. Divide the chosen meshes into several groups based on geomorphography classification, which is determined for each 250m mesh. 3. Select at random almost same numbers of meshes from each of mesh groups.

## 4. Results

“Immediate estimate” by inputting ground motion distribution for the Mw 7.3 earthquake into the fragility functions used in damage estimates by Japan Cabinet Office (2012) overestimated the number of damaged houses by around four times of that reported for the whole suffered area. Several cases are examined for different information. The case the presented method works well is that using both information of Mashiki town, which represents most severely damaged areas, and that of Higashi-Ku, Kumamoto City, which represents typically suffered areas. The numbers of damaged houses read from ten meshes of each area can update the estimate to close to the reported numbers. On the other hand, in a case using information of twenty meshes only from Mashiki town the damage is still overestimated, and in a case with twenty meshes only from Higashi-Ku, Kumamoto City, the number is rather underestimated.

## Acknowledgements

This research was partially supported by the Council for Science, Technology and Innovation (CSTI) through the Cross-ministerial Strategic Innovation Promotion Program (SIP), titled "Enhancement of social



resiliency against natural disasters" (Funding agency: JST). We are grateful to the JMA for providing the data observed at the JMA and local government stations.

Keywords: Kumamoto Earthquake, Bayesian updating, post-earthquake assessment

## Tomographic and gravimetric signatures of the fault system associated with the 2016 Kumamoto earthquake (M7.3), Japan

\*ZHI WANG<sup>1</sup>, Yoshio Fukao<sup>2</sup>, Ayumu Miyakawa<sup>3</sup>, Akira Hasegawa<sup>4</sup>, Yasuko Takei<sup>5</sup>

1. Key Laboratory of Marginal Sea Geology at South China Sea Institute of Oceanology of CAS of China, 2. CEAT, Japan Agency for Marine-Earth Science and Technology, Yokohama, Japan, 3. Geological Survey of Japan, AIST, Tsukuba, Ibaraki, Japan, 4. Department of Geophysics, Tohoku University, Sendai, Japan, 5. Earthquake Research Institute, University of Tokyo, Tokyo, Japan

A series of shallow large earthquakes with the M<sub>j</sub>7.3 mainshock (April 15, 2016) struck the Kumamoto area of Kyushu, Japan. The mainshock was a slip along the Futagawa Fault, a segment of the EW-running Oita-Kumamoto Tectonic Line. By this tectonic line the Beppu-Shimabara Graben is bounded sharply on the south, where NS-extensional crustal deformation is now taking place and earthquakes (including the 2016 aftershocks) are largely NS-dipping normal faulting. We conducted a seismic tomographic study for the crustal V<sub>p</sub> and V<sub>s</sub> anomalies using arrival time data from the Hi-Net stations in Kyushu. The most outstanding tomographic feature in this region is a belt of low V<sub>p</sub> and V<sub>s</sub> anomalies at depths of the upper crust geographically coinciding with the Beppu-Shimabara Graben (Fig.1). This belt is characterized by such an approximate equality that  $dV_s/V_s \approx dV_p/V_p$  ( $<0$ ) in marked contrast to the relation in other regions or at greater depths where  $dV_s/V_s < dV_p/V_p$  ( $<0$ ). This observation can be interpreted in terms of water-saturated, oblate-spheroid pores created by the extensional deformation of the upper crust in the Beppu-Shimabara Graben. The approximate equality between  $dV_s/V_s$  and  $dV_p/V_p$  holds if the aspect ratio  $\alpha$  of pore geometry is either  $\sim 0.04$  (flat pore) or  $\sim 1$  (spherical pore). Once  $\alpha$  is specified, the water volume fraction and hence density anomaly  $d\rho/\rho$  ( $<0$ ) can be calculated from the observed  $dV_p/V_p$  or  $dV_s/V_s$ . We calculate Bouguer anomalies from the density anomaly distribution so obtained. The Bouguer map calculated for spherical pores shows a remarkable negative anomaly belt in agreement with the Beppu-Shimabara Graben signature on the observed Bouguer map (Fig.2). The agreement is very poor if pores are flat. This result demonstrates a unique role of gravity data when it is combined with seismic P and S wave data. The Oita-Kumamoto Tectonic Line, including the Futagawa Fault, is a bimaterial boundary, to the north of which the material is slower in both V<sub>p</sub> and V<sub>s</sub> and less dense. The rupture process of the 2016 Kumamoto earthquake was likely to be affected by this bimaterial nature of the fault.

Keywords: 2016 Kumamoto earthquake, Fluid intrusion, Multiple parameter imaging

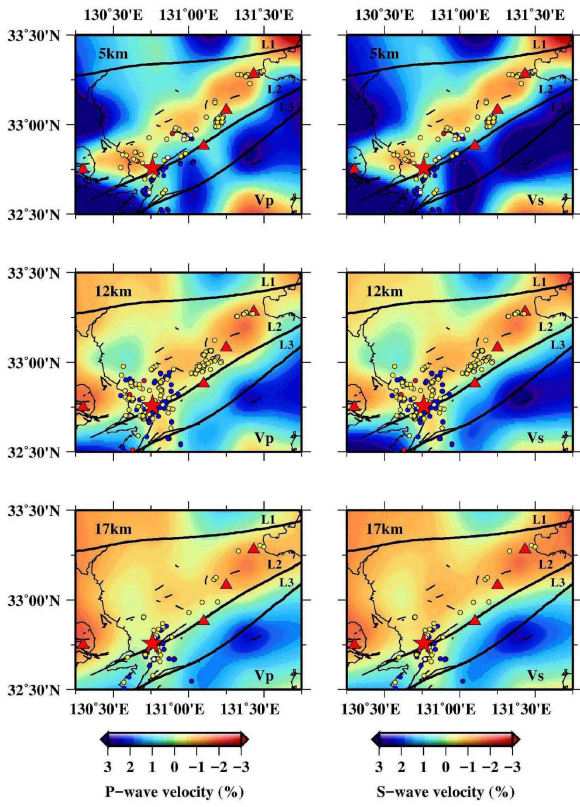


Figure 1:  $V_p$  and  $V_s$  anomalies at three depths of the upper crust

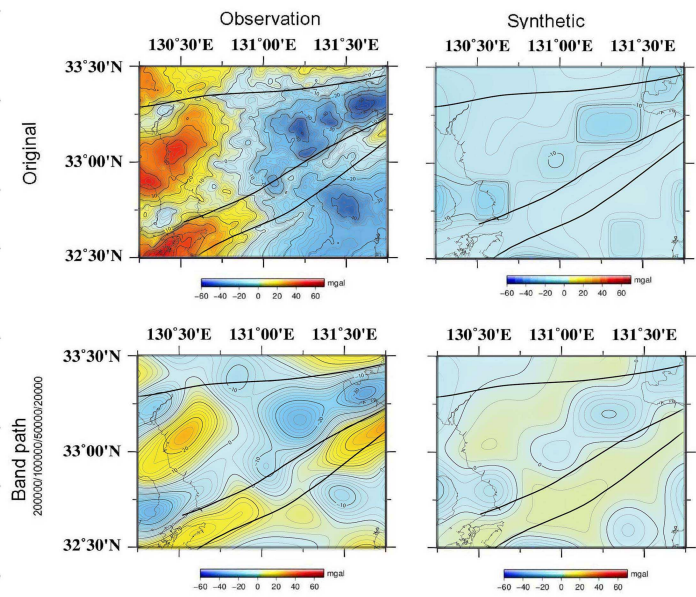


Figure 2: Observed and synthetic Bouguer anomaly maps. Synthetic maps are shown for a case of water-saturated spherical pores. Top: unfiltered maps. Bottom: bandpass-filtered maps.

## Earthquake-volcano interactions in the 2016 Kumamoto earthquake area

\*Dapeng Zhao<sup>1</sup>, Zewei Wang<sup>1</sup>, Xin Liu<sup>1</sup>, Yukihisa Nishizono<sup>2</sup>, Hirohito Inakura<sup>2</sup>

1. Department of Geophysics, Tohoku University, 2. West Japan Engineering Consultants, Inc.

The 16 April 2016 Kumamoto earthquake (M 7.3) took place in north-central Kyushu where several active arc volcanoes exist (e.g., Aso, Kuju, Tsurumidake, and Unzen) due to the active subduction of the Philippine Sea (PHS) plate beneath the Eurasian plate. On 8 October 2016 the Aso volcano erupted, which may be related to the occurrence of the Kumamoto earthquake. Many previous studies have suggested that earthquakes and volcanoes can interact with each other in subduction-zone regions. To investigate the possible earthquake-volcano interaction in Kyushu, in this work we study the three-dimensional seismic velocity ( $V_p$ ,  $V_s$ ) and attenuation ( $Q_p$  and  $Q_s$ ) structures in the source area of the 2016 Kumamoto earthquake (M 7.3) using  $\sim 62,000$  P and S wave arrival times and 48,000  $t^*$  data measured from digital seismograms of 742 local shallow and intermediate-depth earthquakes recorded by the Hi-net stations in Kyushu Island. Our results show that significant low-velocity (low-V) and low-Q (high attenuation) anomalies exist in the crust and mantle wedge beneath the volcanic front and back-arc area, which reflect hot and wet anomalies caused by convective circulation in the mantle wedge and fluids from the PHS slab dehydration. The PHS slab is imaged clearly as a high-velocity (high-V) and high-Q (low attenuation) dipping zone in the upper mantle. The 2016 Kumamoto earthquake occurred in a high-V and high-Q zone in the upper crust, which is surrounded and underlain by low-V and low-Q anomalies in the lower crust and upper mantle. These results suggest that the 2016 Kumamoto earthquake took place in a brittle seismogenic layer in the upper crust, but its rupture nucleation was affected by fluids and arc magma ascending from the mantle wedge. In addition, a prominent low-V and low-Q zone is revealed in the forearc mantle wedge beneath Kyushu, which reflects serpentinization of the forearc mantle due to abundant fluids from the PHS slab dehydration. These results suggest that arc magma and fluids play an important role in the generation and nucleation processes of large crustal earthquakes which can in turn rupture the active faults and produce new cracks in the crust, facilitating the volcanic eruption. As a result, earthquake-volcano interactions take place in north-central Kyushu.

Keywords: Kumamoto earthquake, volcanoes, Kyushu, subduction zone, Philippine Sea plate

## Yufuin fault cause an earthquake with an intensity of lower 6 in Beppu

\*tatsurou yoshimura<sup>1</sup>

1. Meidai Co., Ltd.

Another earthquake of M5.7 occurred in the Oita Prefecture central part 32 seconds after the main shock on April 16, 2016. The intensity 6 lower was observed in Beppu City and the Yufuin city of the northeast about 80km from Kumamoto. Ufuin fault is distributed in aftershock area in the Oita Prefecture central part. The setting of the active fault length was examined by the comparison between scenario magnitude from  $\gamma$ -ray survey results and actualy occurred magnitude.

Keywords: Earthquake in the Oita Prefecture central part, Yufuin fault, Fault length